MEASUREMENT AND ANALYSIS OF THE WIND INDUCED VIBRATION OF A TALL STACK

Michael A. Porter
Dynamic Analysis
Leawood, Kansas 66206

Robert D. Blevins
Consultant
San Diego, California

Dennis H. Martens
Black and Veatch Pritchard
Overland Park, Kansas

ABSTRACT

Field observers reported that two 260-ft (80 m) high stacks of a sulfur recovery plant exhibited significant levels of vibration in winds with velocities between 35 and 45 ft/sec (10 and 13m/sec). A static and dynamic Finite Element (FE) analysis of the stack was conducted to determine the natural frequency and stress in the stack. A flow-induced vibration analysis indicated that the vibration would occur at the coincidence of the vortex shedding frequency with the predicted natural frequency (0.5 to 0.7 Hz) of the stack. Field measurements were conducted to quantify the natural frequency and damping of the stack by exciting the stacks with an attached cable and then measuring the rate and frequency of the free decay. These measurements confirmed the natural frequency predicted by the FE analysis. The measured damping factor of between 0.015 and 0.009 corresponds to a predicted response amplitude near the observed 0.5-ft (0.2 m) vibration amplitude. Analysis of the stresses in the stack and a field inspection showed that this level of vibration is not damaging to the stack or refractory lining.

INTRODUCTION

Field observers reported two 262-ft. (80 meter) high stacks of a sulfur recovery plant as having significant vibrations when the wind velocity was between 35 and 45 ft/sec (9 to 11 m/sec). The stacks displayed the classic vortex-induced movement direction: perpendicular to the wind. The movements of the two stack were observed to be nearly identical.

The stacks have a diameter of 14-ft. diameter with steel thickness ranging from 2.5 inches thick at the bottom to 0.39 inch thick at the top. They were designed to ASME STS-1 criteria. The stacks were fabricated in flanged sections about 50 ft in length. There are 36 anchor bolts, each 100-mm in diameter using a typical chair design at the base.

The stacks are lined with a 3 inches thick, 138-pound/cubic foot refractory material. The refractory was installed with circumferential expansion joints at each flanged section to allow for differential longitudinal expansion between the refractory material and the steel shell. The typical flue gas operating temperature is 1200 degrees F and the stack metal temperature range is 350 to 600 degrees F.

The original field observers were not able to quantify the magnitude stack displacement during the vortex-shedding induced vibration. However, the observed stack movements were deemed significant enough to warrant review of the stack design. The review of the original stack calculations confirmed the design was in agreement with the ASME STS-1 (1992) criteria. The ASME STS-1 suggested damping coefficient for a refractory lined stack had been used in the original calculations.

In order to confirm the continued operability of the stacks, it was decided to:

- conduct field tests to establish actual stack natural frequencies and damping coefficients
- conduct a thorough inspection of the stacks for vibration damage
- conduct a detailed finite element and vortex-induced vibration analysis of the stacks

This paper describes the field measurements, inspections and the analyses that were conducted to confirm the continued operability of the stacks. The Field Measurement and Inspections sections contain details of the field effort. The Finite Element section describes the computed natural frequency and stress analysis effort. The Vortex-Induced Vibration section details the flow-induced vibration analysis as well as the measured natural frequencies and damping values. The results of the field measurements and the various analyses are compared to each other and to the published literature.

FIELD MEASUREMENT

The field damping measurement was conducted by attaching a ¼ inch wire rope to a lifting lug at the top of the stack. A 1-inch rope was

attached to the end of the cable and a small cap-stand type winch was used to pull on the cable using the attached rope. The winch was located at grade about 260 feet from the first stack, providing about a 45 degree included angle between the stack and the wire rope. The stack was excited by using the winch to provide about a 1,000-pound force on the cable and then applying a down pull on the rope by hand. The direction of the pull was in line with the two stack breaching openings.

Although it was possible for one man to excite the stack to some extent, 4 men working in unison were required to obtain motion amplitude that was significantly above the ambient. The stack did not become excited until the wire rope formed a sine wave, which indicated that a standing wave in the rope had been excited. This resonant condition amplified the force provided to the stack by the men. After a steady-state motion had been achieved, the wire rope was released from the winch so that the stack was free to move without external loading.

The stack vibration was measured at the highest access platform level, about the 160 foot above the stack base. Two accelerometers mounted at 90 degrees to each other on the stack wall were used to sense the motion. The accelerometer output was recorded for later analysis on a digital recorder. It took three attempts to excite the first stack at its natural frequency. Data were recorded for all attempts, but only one attempt resulted in amplitudes sufficient to provide useable data for analysis.

Attempts to excite the second stack were not successful. For this stack, the winch was placed about 330 feet from the stack base. The rational for this change was that it would provide greater leverage on the top of the stack and thus increase the amplitude of motion. However, the pull cable never achieved the sine wave movement noted in the excitation of the first stack. In hindsight, it is clear that the geometry of the pull cable on the first stack resulted in a fortunate coincidence of the cable and stack natural frequencies, resulting in greater motion. The change in geometry for the second stack eliminated the excitation of the standing wave in the wire rope.

INSPECTIONS

The inspections of the stacks were conducted using visual, bolt torque checking and Liquid Penetrant (LP) methods. The refractory was inspected visually by use of a man-basket lowered through the stack by a crane. The refractory did not display compression cracks or any damage that could be attributed to the vortex-induced vibration. Only minor refractory damage (surface spalling) was noted; no repair was required.

The steel surface was inspected in the highest stress areas of the anchor chair and breaching opening of both stacks utilizing LP. No crack indications were found. The grout was visually inspected and found to be in good condition with no indication of stack base plate movement.

The anchor bolts of both stacks were inspected using an established bolt load inspection procedure. The first stack anchor bolts were confirmed to be within the procedure-established parameters. The inspection of the second stack's anchor bolts found about 1/3 of the bolts to be under-torqued. The anchor bolts' torque was re-established per the inspection procedure. There was no indication that the under-torque condition of the anchor bolts was due to excessive bolt stress, as there was no damage or deformation of the anchor chair assembly or the grout. The conclusion was that the under-torque condition was from the original construction work.

The flange bolting for both stacks was inspected using a similar procedure. This inspection procedure required four bolts of each flange to be checked. None of the flange bolts were found to be under-torqued. Although it was only possible to check about 75% of the flanges (due to wind and crane availability), the conclusion was that no flange bolt damage had occurred. Visual inspection indicated no movement or cracking of the flanges.

FINITE ELEMENT ANALYSIS

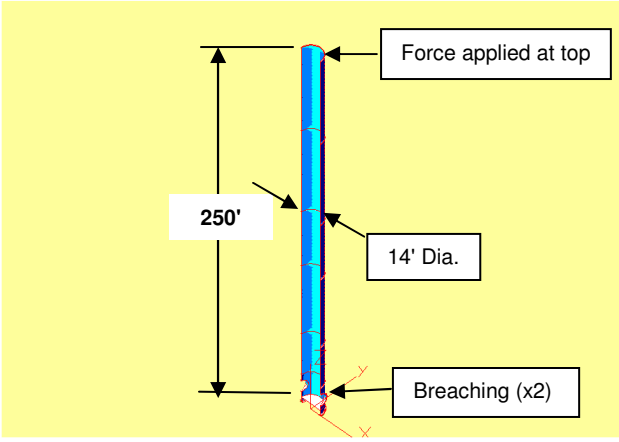

Figure 1- Cut-Away View of Stack

Two initial FE models of the stack were originally constructed. Both models had essentially the same geometric configuration as illustrated in Figure 1. The primary difference between the two models was that one of the models assumed that the refractory would contribute to the stiffness of the stack and the other model assumed no stiffness contribution from the refractory. No direct measurement of the stack stiffness was conducted in the field. However, from the field measurement data it was possible to determine the natural frequencies of the stacks. From this data, we can also deduce the apparent stiffness of the system.

Natural Frequencies

The original static models (T2 & T3) were used to construct corresponding dynamic models (T2D & T3D). The natural frequencies of the stack were computed using these models. The computed natural frequencies for the first two modes are indicated in Table 1, along with the frequencies determined from the field data.

From the data in Table 1, it is clear that the frequencies computed using model T3D (the model which does not include the stiffness of the refractory) are closer to the actual measured frequencies than those computed using model T2D. In fact, if the mass of the platforms and other miscellaneous items were added to model T3D, the computed frequencies would be even closer to the measured values. The good agreement between the computed and measured natural frequencies is an indication that the stiffness of model T3D (and correspondingly T3) is representative of the actual stack. Note that the vibration mode frequency in the East-West direction is lower than in the North-South direction due to the softening effect of the dual breach openings in the East-West direction. The FE model, which does not include the stiffness contribution of the refractory (T3), appears to best fit the field data. Thus, in subsequent analyses, we used only the stiffness of the steel in the computations. The refractory has been included as mass only.

Wind Load (Dynamic) Stress

Since it was clear from preliminary analyses that the regions of highest stress would occur in the lower section(s) of the stack, the models used had a more refined mesh in the base section than in the upper sections. In addition, the pre-load tension in the bolts was set to approximately 16,000 psi and the contact between the base of the stack and the concrete pad was modeled as a compression-only connection. Because the location of the compressive contact region (between the stack base and the concrete) changes with the direction of the load, three models were required.

To arrive at an equivalent stack load representing the dynamic wind loading, the dynamic wind force was first computed using the procedure outlined by Blevens (1990). This force was then multiplied by a dynamic amplification factor based on an assumed viscous damping ratio of 0.0066. The computed load was then applied in a horizontal direction to the top of the stack. This load resulted in a moment of approximately 27,000,000 FT-LB at the base of the stack. This moment induced by this equivalent static load was slightly larger than the design 90-mph wind load of 24,867,000 FT-LB.

The deflection computed at the top of the FE stack model due to the equivalent static load ranged from approximately 16.5" to 19" depending on the direction of load application, i.e. the deflection was greatest when the load was applied in the direction of the breaching openings. In the field, the observed maximum stack displacement due to wind was approximately 6 inches. Thus, the computed deflections were approximately three times the observed deflections. The reason for this difference involves both the actual damping in the stacks and the dependency of this damping on system displacement amplitude, as will be discussed in the Vortex-Induced Vibration Analysis section.

In a linear system, the stresses are directly proportional to the applied loads. Thus, the computed stresses using the FE models were probably overstated by a factor of 3. The location of the highest stress regions, however, should stay the same. This insight was a useful tool in identifying the regions where indications of excessive stress might be expected. These regions were used to determine field visual and liquid penetrant inspection locations.

Figure 2 illustrates the indicated stresses in the base section of the stack due to a load applied in the North-South direction. Note that the axis of the inlet breaching runs in the East-West direction, making the North-South direction the "strong" direction for the stack in bending. In Figure 2 we see that the highest indicated stresses in the shell are

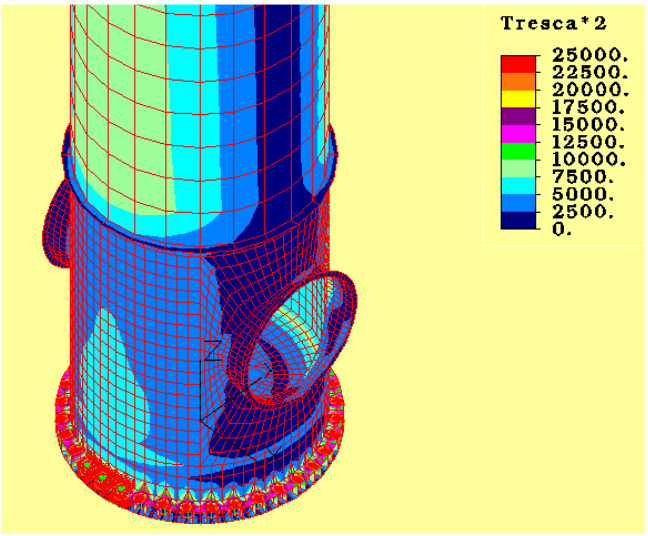

Figure 2 - Dynamic Wind Load Stress Intensity

near the nozzle intersections. Even without taking the factor-of-3 excess in the load into account, the indicated stresses in the shell are not of concern.

Figure 3 provides a more detailed look at the portion of the chair where the bolts are attached. The stresses in the stiffener between the upper and lower rings of the chair are indicated to be on the order of 24-26,000 psi. If the actual loads in the field had been as high as those used for this model, we would have expected to see some

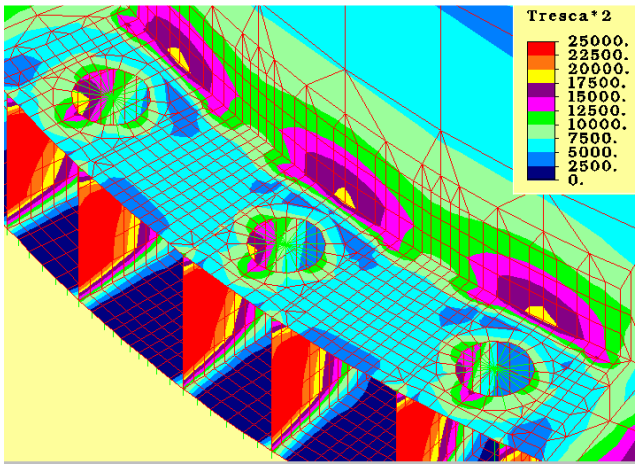

Figure 3 - Stress Intensity in Chair

evidence of over-stressing in the weld areas around these stiffeners. A good indication that the equivalent static loads applied to the model were conservative is the fact that no such damage was observed is.

In summary, since the magnitude of the applied loads on the FE models was high by nearly a factor of 3, the indicated stresses are also high by that factor. Thus, where the indicated stress is 24,000 psi, it is more likely to be on the order of 8,000 psi. The fact that no indications of cyclic stress-induced problems were found in the existing stacks is a good indication that the loads and resultant stresses in the models are overly conservative. Thus, it was concluded that the

dynamic, wind induced stresses should pose no problems for the stacks.

Design Wind Load (Static) Stress

The design wind load of 90 mph produces a moment of 24,867,000 FT-LB at the base of the stack. This load has been applied to a model in the East-West direction (which is the weakest direction of the stack) in order to evaluate the stresses in the stack due to this design load.

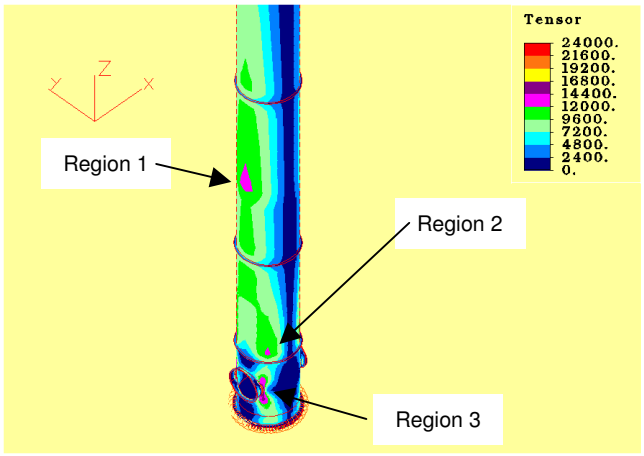

Figure 4 - High Stress Regions

Figure 4 presents a view of the areas where the highest stresses are indicated. The stresses indicated on the model are the longitudinal compressive stresses due to the combination of the dead load and the bending load due to the wind.

The three regions where the highest stresses are indicated are marked as regions 1, 2 and 3. Region 1 is on the third section from the bottom, Region 2 is on the second section from the bottom and Region 3 is on the base section. The wall thickness of these regions and the allowable stress is presented in Table 2. Note that these allowable stresses are from the AISC manual as dictated by ASME-STS-1-1992, 4.6.1.

The AISC procedure requires that the compressive stress due to the dead load and those due to bending be evaluated separately. The two loads are compared to the code requirements individually and the resultant ratios are summed. The sum must be less than unity.

Figure 5 illustrates the compressive stresses due to the dead load of the stack. Figure 6 illustrates the compressive stress due to the wind induced bending. Note that the effect of the nozzle opening is to develop a stress concentration region along the vertical sides of the nozzle in the base section. In addition, a stress concentration is indicated in the section above the base section. This is true for both the dead load of the stack (Figure 5) and the wind load (Figure 6).

The stress that has been used for the code comparison (Table 2) is the highest stress indicated, excluding the peak stresses, per AISC 9th Edition, paragraph A5.1. In the case of Regions 1 and 2, the highest indicated stress for the color indicated has been used. For Region 3 (around the nozzles), the stresses within approximately two thicknesses of the intersection have been considered peak, in accordance with the paper by Porter and Martens (1996) that evaluates the stresses at a nozzle intersection. In all cases, the indicated stresses due to the design wind load are below the AISC allowables.

VORTEX-INDUCED VIBRATION ANALYSIS

In order to confirm that the worst case of wind loading had indeed been identified, a classical flow-induced vibration analysis of the stack was conducted.

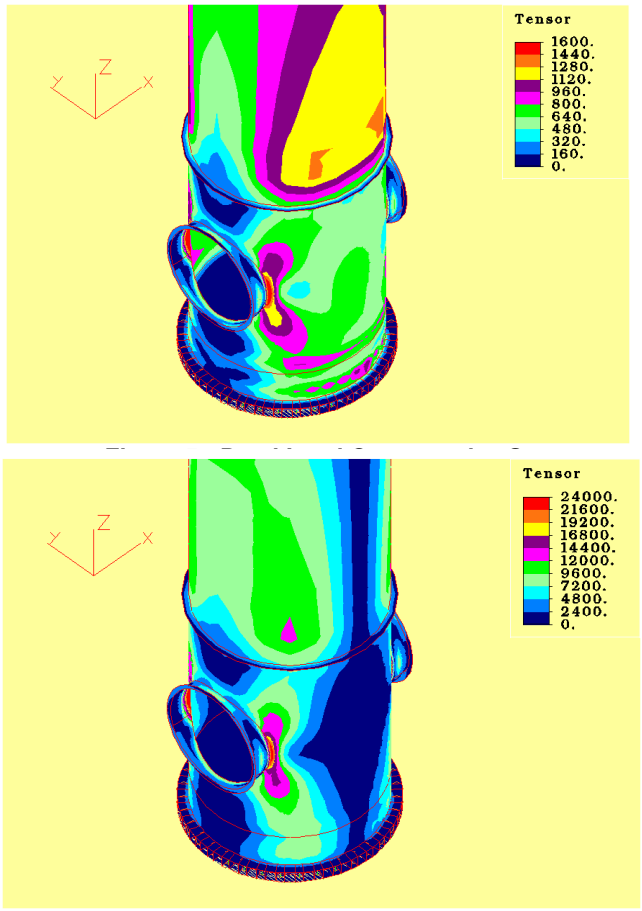

Figure 6 - Wind Induced Bending Stress

Theory

Vortices are shed by the wind over the stack. When the shedding frequency approaches a natural frequency of the stack, the vortices can lock onto the stack natural frequency and induce vibrations that are primarily perpendicular to the wind (Blevins, 1990). The shedding frequency is a function of Reynolds number, wind speed, and stack diameter.

The amplitude of the resonant, locked-in stack vibrations are limited by mass and damping.

The ASME Steel Stack Standard (1992) provides representative values for damping of lined stacks. The low value is $\zeta = 0.0032$, the average value is $\zeta = 0.0067$, and the high value is $\zeta = 0.010$. These values are consistent with the measured values of $\zeta = 0.009$ to 0.015 that were determined from the field measurements. The wind-induced vortices have the greatest effect on the top third of the stack. The average thickness of the upper third of the stack is 1 inch. Combining the mass of the steel shell (density of 0.289 LB/cu in) with 3 inches of

refractory (density of 138 LB/cu ft) results in a stack mass per unit length (m) of 277 LB/in or 3324 LB/ft.

At 30mph (U = 44 ft/sec) in ambient air (kinematic viscosity, ν=0.001 ft2/s) the Reynolds number (Re) of the 13.9 ft stack diameter (D) is: Re = UD/ν = 6.12e6. In this range the Strouhal number is S=0.23. These numbers may then be combined to produce the indicated vortex shedding frequency of:

$$f_s = SU/D = 0.73 \text{ Hz}$$

Using the same Strouhal number and the measured natural frequencies of 0.54 and 0.60 Hz, the computed resonant wind velocities are 32.6 and 36.3 ft/s. These are close to the 35 to 45 ft/s range where stack vibration was observed.

The amplitude of resonant vortex-induced vibration is limited by the reduced damping parameter, which is a function of air density (ρ=0.075 lb/ft^3), stack mass per unit length, diameter and damping factor. This gives,

$$\delta_r = 2m(2\pi\zeta)/\rho D^2 = 25.9 \text{ to } 43.2$$

for damping factors of 0.009 to 0.015. The above correlation for the resonant amplitude is taken from Blevins (1990). For the simple harmonic model with a lift coefficient C_L of 0.5 the predicted amplitude is,

$$Ay = DC_L/(4\pi S^2 \delta_r) = 0.24 \text{ to } 0.4 \text{ ft}$$

The semi-empirical wake oscillator model, applied to a cantilever, gives a tip amplitude of 0.32 to 0.55 ft. These amplitudes are close to the observed 0.5-ft amplitude.

Analysis of Field Data

The FE analysis indicated that the natural frequency of the stacks would range from about 0.55 to 0.77 HZ depending on the direction of motion and the assumed stiffness of the refractory. It was assumed that the stack had a characteristic damping coefficient of 0.0066 and that the stack would respond to a harmonically applied force (vortex shedding from the wind) in a linear fashion. Using these values, a static load was developed to simulate the dynamic effect of a 30-mph wind on the stack. The field data provide useful insight concerning the validity of these assumptions.

Stack Natural Frequency

In general, the data analyzed has provided ample information concerning the natural frequencies of the stacks. The first modal frequency in the East-West direction was found to be approximately 0.54 Hz. In the North-South direction, the measured natural frequency was approximately 0.60 Hz. Figure 7 illustrates a typical plot of the measured response in the East-West direction. The modal frequencies corresponding to first mode motion in the East-West and North-South directions have been labeled. In addition, the components associated with the second mode motion have been identified.

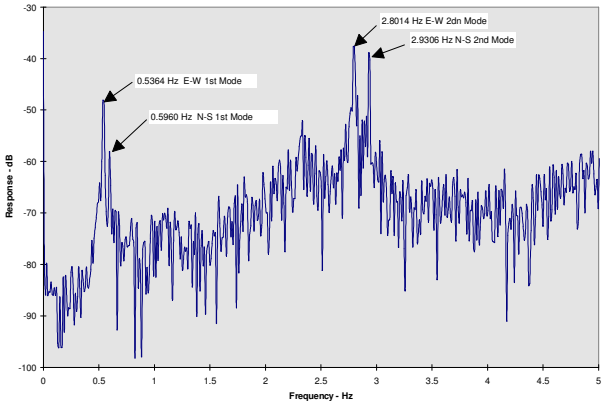

Figure 7 - East-West Spectrum Plot

The appearance that the second mode motion is greater than the first mode motion is due to the combination of the unit used for the measurement (acceleration) and the low frequency roll-off of the recording system. If the data were plotted in terms of displacement instead of acceleration, the second mode magnitude would drop by about 20 dB (a factor of 10) relative to the first mode. Correcting for the recorder response as well, we find that the first mode motion is approximately 100 times the magnitude of the second mode motion. No specific reference for the magnitude is indicated due to uncertainties in the recorder gain setting during the measurement process. It is estimated, however, that the motion at the upper platform level was on the order of 1-1.5" (peak) during the measurement process.

Stack Damping

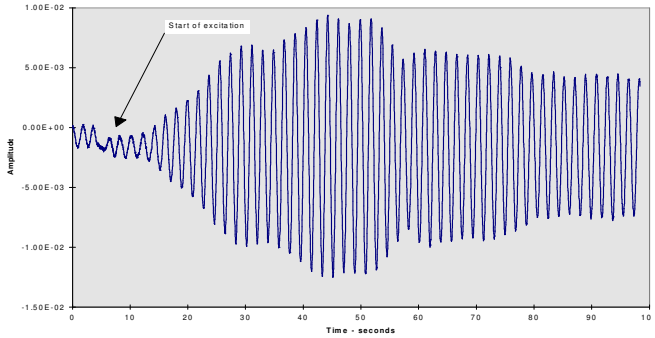

Figure 8 - Time Signal - Filtered

It had been hoped that by exciting the stack with the cable, a record of the decay in motion of the stack could be used to compute the damping. The data collected, however, did not reveal a clear pattern. Figure 8 illustrates a portion of the amplitude vs time signal, which begins just before the excitation, started. Note that this signal has been passed through a filter to remove all but that portion centered on 0.54 Hz.

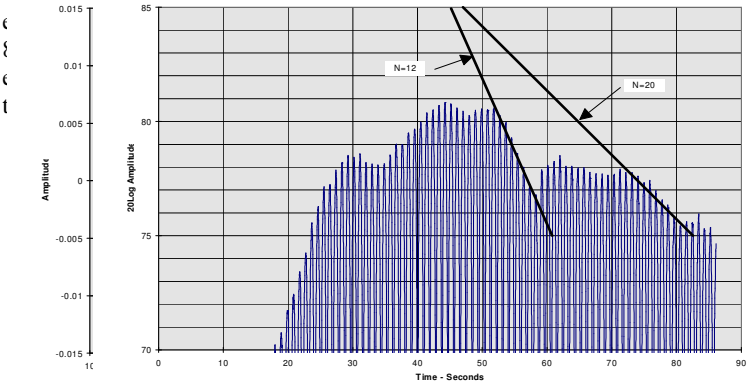

Figure 10 - Log Plot of Time Signal

If viscous damping controls the amplitude of the stack motion, we would expect to see an exponential decay in the amplitude. On the other hand, if coulomb (friction) damping were controlling, we would expect to see a linear decay in the amplitude with time. Neither case is clearly evident. However, we may at least bracket the level of damping in the system using a technique that is commonly used in acoustic analysis.

The most common method of extracting the damping from a time decay signal is called the "log decrement" method. The log decrement (δ) is defined as:

$$\delta = \ln\left(\frac{y_1}{y_2}\right)$$

Where y_1 and y_2 are the amplitudes of two successive oscillations of the signal.

If the damping is small ($\zeta > 0.1$), then the critical damping ratio (ζ) is related to the log decrement by:

$$\zeta = \frac{\delta}{2 * \pi}$$

If the signal is plotted with a logarithmic scale, it may be shown that:

$$\zeta = \frac{0.183}{N}$$

Where N is the number of cycles required for the signal to decrease by 10 dB (a factor of approximately 3.16).

Plotted on a logarithmic scale, an exponential decay would form a straight line. Therefore, by drawing a straight line through the decay and then counting the number of cycles that was required for the line to change 10 dB, we may compute the damping.

Figure 10 illustrates the same portion of the signal that was shown in Figure 9. The only difference is that Figure 10 uses a logarithmic vertical scale. There are two distinct regions of decay in this portion of the signal. A straight line passing through the first decay segment indicates that the signal would take approximately 12 cycles to decay by 10 dB. A line passing through the second decay segment indicates that the signal would take approximately 20 cycles to decay 10 dB. Using the equation above, the respective damping values would be 0.015 and 0.009 respectively.

The fact that the damping value appears to be greater for the first line than for the second is consistent with coulomb (friction) damping. That is, the damping is proportional to the amplitude; the greater the amplitude of motion, the greater the friction. From these data points, we conclude that the average damping ratio is on the order of 0.009-0.015.

Another indication of the damping in the system is the response of the stack to wind excitation. On one occasion, the gross motion of the stack(s) caused by a wind with a velocity of approximately 40 ft/sec was carefully observed. The observed maximum amplitude of the stack due to this wind excitation was approximately 6" peak (12" peak-to-peak). Since the vortex shedding frequency for this wind speed is about the same (or slightly higher) than the natural frequency of the stack, we would expect the stack to be excited.

The amplitude of the motion, according to Blevins (1990), is primarily a function of the damping in the stack. Figure 11 illustrates the amplitude of motion that would be expected in the stack as a function of the damping. Three different curves are plotted, representing the range of prediction schemes that have been proposed, according to Blevins. The solid horizontal line indicates the displacement observed on the subject stacks. From Figure 8, we may deduce that the damping in the stacks is on the order of 0.008 to 0.012, about the same as measured in the field. This is consistent with the range of damping ratios of 0.0086 to 0.0138 suggested by Blevins (p330), based on field measurements of other stacks.

The stress produced by these amplitudes is estimated from the finite element model. The modal analysis gives a relationship between the stress in the base of the stack and the tip amplitude when it is excited in a single mode. For a tip amplitude of 0.5 ft this gives a stress of 8,000 psi, which is well below the fatigue limit for the material.

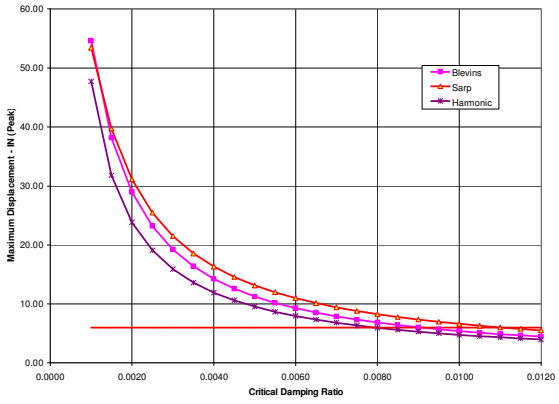

Figure 11 - Predicted Amplitude vs Damping Ratio

CONCLUSIONS

The conclusions of this study are:

1. A 262-ft tall, 13.9-ft diameter stack was observed to vibrate in the wind with tip amplitude of approximately 0.5 ft.
2. The natural frequencies and damping of the stack were measured by attaching a cable to the stack, pulling on the cable to generate stack motion and than releasing the cable. The measured natural frequencies are 0.54 Hz in the East-West mode and 0.6 Hz in the North-South mode. The measured fractions of critical damping were between 0.009 to 0.015.
3. A detailed finite element of the model was made. This model showed that the stack is predicted to be capable of withstanding the mean wind loads.
4. A vortex-induced vibration analysis shows that the stack is predicted to be resonant with vortex shedding for wind speeds between 35 and 45 ft/sec and the predicted amplitudes are between 0.25 to 0.55 ft. The predicted stresses are within the fatigue endurance limit of the stack.

REFERENCES

ASME STS-1-1992, Steel Stacks, ASME, N.Y., 1993.

Blevins, R.D., 1990, *Flow-Induced Vibration*, 2nd Ed., Van Nostrand Reinhold, N.Y.

Porter, M. A. and Martens, D. H., 1996, "A Comparison of the Stress Results from Several Commercial Finite Element Codes with

ASME Section VIII, Division 2 Requirements", PVP Vol. 336,
ASME, pp 361-371

Table 1
Computed and Measured Natural Frequencies - Hz

	Source		
	Model T2D	Model T3D	Field Measurement
N-S Mode	0.77	0.62	0.60
E-W Mode	0.69	0.55	0.54

Table 2
Design Wind Load Stresses

Region	Thickness	Allowable Compressive Stress - Fa	Allowable Bending Stress - Fb	Computed Dead Load Stress - fa	Computed Bending Load Stress - fb	Code Ratio Sum
1	1.014	10,059	22,070	1000	15,000	0.78
2	1.014	10,059	22,070	1400	15,000	0.82
3	2.264	9,988	22,070	1400	18.000	0.96